Nanoparticle Detection

DOI: 10.1002/anie.201305962

Nanoparticle-Imprinted Polymers for Size-Selective Recognition of Nanoparticles**

*Shlomit Kraus-Ophir, Julia Witt, Gunther Wittstock, and Daniel Mandler**

Abstract: *Citrate-stabilized gold nanoparticles 15 nm and 33 nm in diameter were transferred concomitantly with a monolayer of positively charged polyaniline by Langmuir–Blodgett transfer at pH 5 onto a conducting indium-doped tin oxide (ITO) support. Films consisting of one to three layers of polyaniline with thicknesses of 1–3 nm were prepared and characterized by scanning electron microscopy (SEM), atomic force microscopy (AFM), and X-ray photoelectron spectroscopy. After electro-oxidation of the Au nanoparticles in 0.1 M KCl, cavities were left behind in the film that could be analyzed by SEM. These cavities were able to recapture analyte nanoparticles from a solution of pH 10 and showed size-exclusion properties. The amount of nanoparticles taken up by the cavities was conveniently analyzed by measuring the charge associated with the electro-oxidation of these particles in 0.1 M KCl after the film had been rinsed with water. The size-exclusion properties improved with the number of Langmuir–Blodgett layers transferred.*

Nanotoxicity is a new scientific discipline[1] which requires the development of appropriate tools for the determination of nanoobjects such as metallic nanoparticles (NPs). These tools are also crucial for monitoring the different interactions between nanoobjects and organisms, such as permeation, accumulation, and chemical transformation. The interactions that determine the nanotoxicity are affected by the core, size, shape, and stabilizing shell[2] of the objects. Consequently, there is a growing need for adequate methodologies suitable for studying the interactions between engineered nanoobjects and interfaces. Approaches have been reported for measuring single particles based on their size.[3] However, simple, miniature, and inexpensive sensors for the detection of specific NPs based on the criteria mentioned above are not available yet.

Here we present a new concept for the selective recognition of NPs by a polymeric matrix imprinted with the same NPs. This material can be considered to be a nanoparticle-imprinted polymer (NIP) in analogy to the well-known concept of molecularly imprinted polymers (MIPs)[2a,4] in which the molecular analyte is imprinted in a polymer by polymerization of appropriate monomers with which it chemically associates. The removal of the template forms complementary cavities capable of selectively recognizing the analyte. Recently, the approach was extended to large molecules such as proteins and living organisms.[5] NIPs as bulk material were introduced by Koenig and Chechik,[6] who used polymerizable ligands to stabilize gold nanoparticles (AuNPs). The ligands were cross-linked and then the Au core was chemically etched. The resulting NIP showed selective sorption of small AuNPs. More detailed investigations revealed the formation of polymeric beads around the template NPs, rather than a continuous matrix.[7] Moreover, there was no attempt to either form thinner NIP films or to use the resulting powder as a sensing tool.

Our approach is directed towards thin NIP films as the recognition element for efficient and fast sensing devices. NPs have been embedded into thin films by diverse methods such as electrodeposition,[8] spin-[9] and dip-coating,[10] and layer-by-layer[11] and vacuum deposition.[12] An appealing approach is the Langmuir–Blodgett (LB) technique, in which nanoobjects can be incorporated into monolayers made of amphiphiles.[13] Two-dimensional nanocomposites composed of an organic LB film and NPs have been assembled by codispersion of the two components,[14] by formation of the NPs directly at the water–air interface,[15] and by electrostatic extraction of the NPs from the subphase into the LB film.[16]

Here, the latter approach was followed. Citrate-protected AuNPs were dissolved in the aqueous subphase (pH 5) of a Langmuir trough. A polyaniline (PANI) layer was spread at the water–air interface. This layer is positively charged at pH 5 while the citrate-protected AuNPs carry negative charges at the same pH. The extracted AuNPs strongly associate with the PANI film to form a preorganized composite at the water–air interface (Figure 1). The Langmuir method offers many advantages for the highly reproducible assembly of composites with precise control over thickness and the surface concentration of AuNPs. The surface pressure, which was used to obtain compact films, verified the extraction of the AuNPs by the Langmuir film (Supporting Information SI.1).

[*] S. Kraus-Ophir, Prof. D. Mandler
Institute of Chemistry, The Hebrew University of Jerusalem
Jerusalem 91904 (Israel)
E-mail: mandler@vms.huji.ac.il
Homepage: http://chem.ch.huji.ac.il/mandler
J. Witt, Prof. G. Wittstock
Carl von Ossietzky University of Oldenburg
Faculty of Mathematics and Natural Science
Center of Interface Science, Department of Chemistry
26111 Oldenburg (Germany)

[**] This work was supported financially by the German Israeli Foundation (research grant no. 1074-49.10/2009) and The Harvey M. Krueger Family Center for Nanoscience and Nanotechnology of the Hebrew University. S. K.-O. acknowledges the support of the Eshkol and CAMBR Scholarships. We thank A. E. Wright (Thermo Fischer Scientific) for expert technical support in performing the XPS measurements.

Supporting information for this article is available on the WWW under http://dx.doi.org/10.1002/anie.201305962.

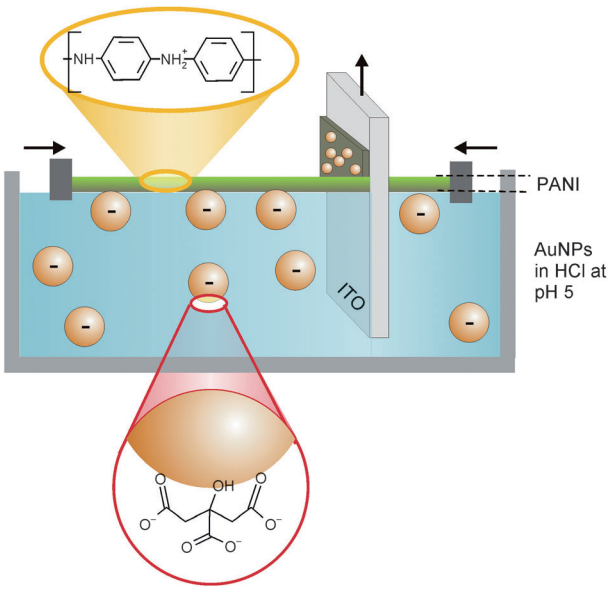

Figure 1. Electrostatic interaction between positively charged PANI and negatively charged AuNPs to form a nanocomposite at the water–air interface that can be transferred onto ITO.

The nanocomposite films were vertically transferred onto an indium-doped tin oxide (ITO) substrate. Successive deposition resulted in multilayers (Supporting Information SI.2). ITO as the solid support allows electrochemical and/or optical stimulation. Figure 2a shows a scanning electron microscopy (SEM) image of the nanocomposite film of AuNPs in PANI (AuNPs@PANI). The well-dispersed randomly arranged AuNPs are clearly visible.

The controlled release of the AuNPs was carried out by electro-oxidation of the metallic gold core in chloride-containing electrolytes to form NIPs. Figure 2b–d shows the cavities imprinted by the AuNPs in two LB-deposited PANI layers. The size of the cavities was usually smaller than the diameter of the AuNPs (Figure 2c), which is conceivable taking into account that the NP diameter (33 nm) was larger than the PANI film thickness, that is, 1 nm for a monolayer; however, it is possible that the PANI was partially folded to form multilayers.[16b] The thickness was confirmed by atomic force measurements in solution (Figure SI.2 in the Supporting Information). Statistical image analysis showed that the diameter of the cavities did not change with the number of layers, as detailed in SI.3 in the Supporting Information. Electrochemical oxidation did not dissolve all the embedded AuNPs as confirmed by X-ray photoelectron spectroscopy (Supporting Information SI.4). Some AuNPs remained chemically unchanged presumably due to the electrical insulation of PANI under the experimental conditions.[17] Another particle population was oxidized but remained within the matrix, even after application of a positive potential ($E = 1.3$ V vs. Ag/AgCl) for 7 h; this is most probably because the PANI film covering the AuNPs hindered chloride access (required for the dissolution).

Figure 3a shows a representative linear sweep voltammogram (LSV) recorded with NIP-coated ITO made of one to three Langmuir layers of the AuNPs@PANI upon removal of

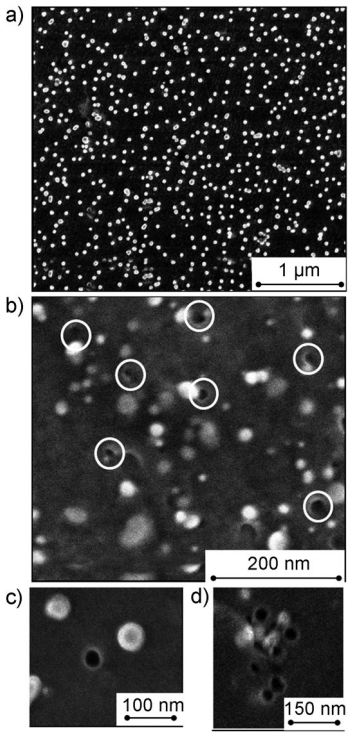

Figure 2. SEM images of two LB layers of 33-nm-diameter AuNPs@PANI nanocomposite deposited at 28 mN m^{-1} before (a) and after (b–d) electrochemical dissolution of gold.

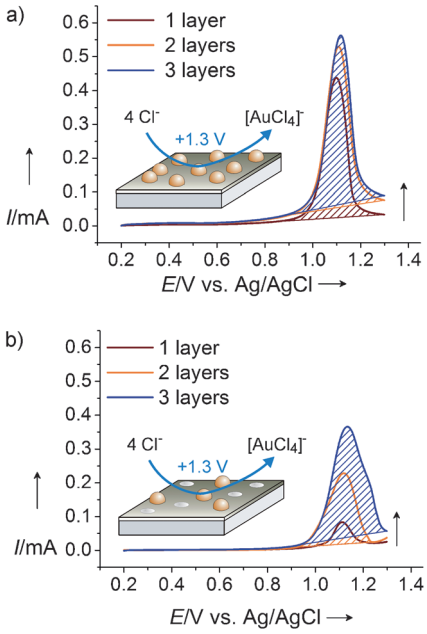

Figure 3. LSV of one to three deposited NIP (33-nm AuNPs) layers recorded in 0.1 M KCl with a scan rate of 50 mV s^{-1}: a) removal of the initially imprinted AuNPs; b) removal of the taken up AuNPs.

the template. The recognition ability of the NIPs was examined by inserting the template matrix in an AuNP-containing alkaline solution (pH 10); since the PANI film is neutral at this pH (Experimental Section in the Supporting Information), unspecific electrostatic attractions between the

polymer matrix and the negatively charged AuNPs are eliminated. After uptake of the AuNPs and gentle washing with water, another LSV was recorded in 0.1 M KCl (Figure 3b) and compared to the LSV for the template removal (Figure 3a). Better insight was possible by comparing the charge densities obtained from integrating the currents with respect to time (Table SI.2 in Supporting Information SI.5 for statistical results and discussion of the significance of this number). The charge density associated with the initial removal of the AuNP templates increased with the number of deposited LB layers due to the accumulative deposition of AuNPs in each layer.[16b] The charge for oxidizing the taken up AuNPs also increased with the number of deposited layers because a layer with more NP templates resulted in a NIP having a higher density of cavities available for uptake. Such a layer will therefore have a higher capacity of the NIP (the description of capacity is discussed in Supporting Information SI.5). In all cases, the oxidation charge density was within the same order of magnitude for both imprinted and taken up AuNPs. This implies a high efficiency for the uptake of the NIPs. Interestingly, the ratio $r = <Q_{\text{analyte}}> / <Q_{\text{template}}>$ between the mean charge densities for the oxidation of the reuptaken analyte AuNPs and the oxidation of the template AuNPs increased with the film thickness. The ratio r indicates the probability of a formed cavity to retain a NP during uptake and immersion in solution. This trend is conceivable as multilayer LB films resulted in deeper cavities that enhanced the interfacial interactions between the NIPs and the AuNPs. It is important to mention that similar, nonimprinted layers of PANI which were immersed overnight in a basic solution of AuNPs did not reveal any gold electro-oxidation, thus illustrating the crucial importance of the template-formed cavities in NIPs. Since PANI is insulating in neutral 0.1 M KCl, only those particles that had an electrical contact to the ITO support were oxidizable. In this way the physically adsorbed AuNPs were not counted and ensured that only AuNPs entrapped in the complementary cavities were counted.

The selectivity of NIPs describes their ability to discriminate between different populations of AuNPs. For a proof of concept, we considered size-exclusion as a primary model factor using two populations of AuNPs with diameters of (15 ± 2.4) and (33 ± 5.4) nm. They were used both as templates during LB deposition and as analytes during uptake. This made it possible to study the ability of NIPs to discriminate by size without the complicated consideration of particle size distributions in solution and after uptake inside the film, for which strictly comparable analytical methods are not available. NIPs were prepared with one to three LB layers. Each NIP was imprinted by one template population and exposed separately to different analyte populations. This study design yielded a total of 12 NIP–analyte combinations (3 layer thicknesses $\times 2$ template NPs $\times 2$ analyte NPs). The NIPs were termed 33-1, 33-2, and 33-3 for films imprinted by the 33-nm-diameter template AuNPs and made of one, two, and three layers, respectively. Correspondingly, we used 15-1, 15-2, and 15-3 for NIPs imprinted by 15-nm diameter templates. The presence of taken up AuNPs was verified and quantified by LSV as described above.

The comparison of the uptake abilities of different NIPs was based on the uptake of differently sized analyte AuNPs by one NIP (Figure 4; the figure shows only the LSV for NIPs made of one and three LB layers; the full set of information is found in Supporting Information SI.6). Figure 4a compares the uptake of either 33- or 15-nm-sized analyte AuNPs by NIPs imprinted by 33-nm diameter templates. In both 33-

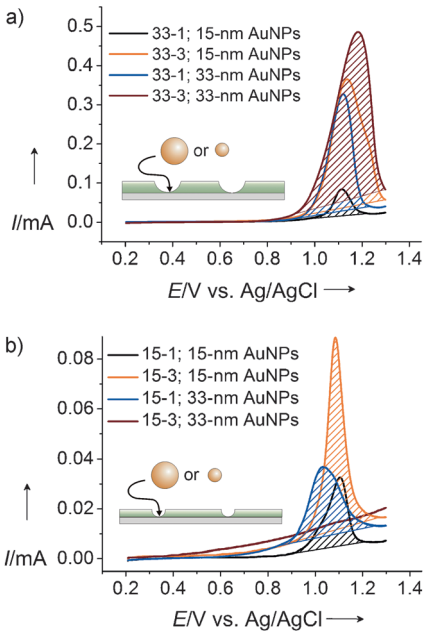

Figure 4. LSV after uptake of 33- and 15-nm AuNPs by one and three layers of NIPs imprinted by a) 33-nm NPs (33-1 and 33-3) and b) 15-nm NPs (15-1 and 15-3).

1 and 33-3 NIPs, the charge associated with the oxidation of the 33-nm analyte AuNPs was higher than that obtained upon oxidation of 15-nm analyte AuNPs. Yet, clear oxidation signals were observed also when the analyte AuNPs were smaller than the template AuNPs. Figure 4b shows the comparison between the uptake of both analytes by one and three layers of NIPs imprinted with 15-nm template AuNPs. For 15-1 the charge measured for the oxidation of the two analyte AuNPs was similar. However, as the number of layers increased, a clear increase of the oxidation charge of the 15-nm analyte AuNPs was observed while the oxidation charge of the 33-nm analyte particles decreased.

The comparison of uptake efficiency based on the oxidation charge of the analyte AuNPs is problematic since the charge resulting from one large particle exceeds that from a small particle. Therefore, we normalized the charges by the calculated charge per particle (Supporting Information SI.7). Figure 5 shows (in a logarithmic scale) the number of analyte AuNPs, N_{uptake}, as calculated from the LSV (including 33-2 and 15-2 NIPs which have been omitted in Figure 4).

For 15-1 to 15-3 (Figure 5a, dark red and orange columns) a significant preference for the 15-nm analyte AuNPs over the larger AuNPs was found, indicating higher affinity towards particles of the same size as the template. Moreover, the

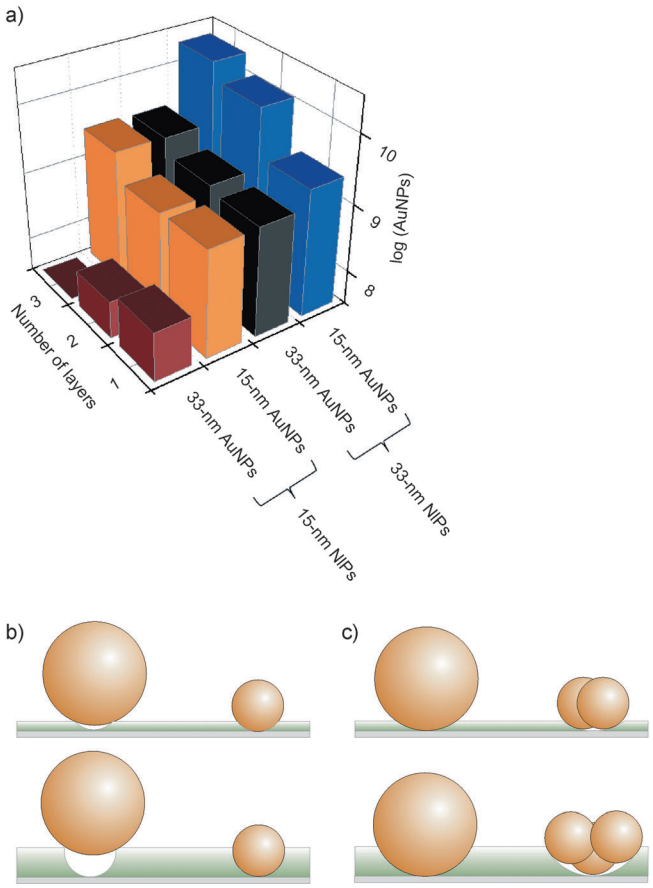

Figure 5. a) Logarithmic plot of 15- and 33-nm AuNPs taken up by NIPs consisting of one to three LB layers imprinted by either 15- or 33-nm AuNPs. b, c) Model of the re-uptake process by the various NIPs showing the effect of the number of layers and imprinted AuNPs.

exclusion of larger particles improved with the increasing number of layers, as is manifested by the increasing ratio between columns. This differentiation in selectivity is attributed to the increasing depth of the cavity; that is, thicker films impeded the uptake of larger AuNPs that could be accommodated in shallower pores (Figure 5b).

In contrast, the number of smaller analyte AuNPs taken up by the 33-1 to 33-3 NIPs (Figure 5a, blue columns) was one order of magnitude higher than the uptake of the larger 33-nm AuNPs used for templating (Figure 5a, black columns). This trend increased with the number of layers and could be explained by the fact that a larger number of small particles can be hosted by a deeper cavity than by a shallower cavity (Figure 5c). In addition, trapped analyte particles were less likely to be detached from deeper cavities upon rinsing.

The two middle columns correspond to the uptake of analyte AuNPs that are the same size as the template. Very similar N_{uptake} values were obtained for these situations indicating the remarkable consistency and homogeneity of the number of cavities produced in the imprinting process and filled during uptake. This results in a uniform recognition capacity of the both NIPs for the analyte NP that has the same size as the template.

To conclude, this work demonstrates for the first time the size-exclusion of nanoparticles by imprinted polymers. In the design of selective nanoparticle-imprinted polymers, template particles should be used that are the same size as the analyte particle. The size exclusion improves with the number of layers, that is, the depth of the cavities. The fact that the AuNPs remain in the holes after the NIPs have been washed hints at the existence of attractive interactions between them and the matrix, that is, PANI. We attribute the latter to hydrogen bonding, which has shown to be of importance in the interactions between AuNPs and a cellulose-based matrix.[18] Evidently, the next step will comprise examining the recognition ability of target NPs from a mixture of two and more populations of different sized particles. However, other analytical methods besides electrochemistry should be considered for evaluating the captured particles, as the latter does not discriminate between large and small NPs. Thanks to this significant accomplishment, other criteria are currently being examined as a means of differentiating nanoparticles based on their shape, shell, and chemical or physical interactions.

Received: July 9, 2013
Revised: August 20, 2013
Published online: November 4, 2013

Keywords: analytical methods · imprinting · nanoparticles · size-selective recognition · thin films

[1] a) V. L. Colvin, *Nat. Biotechnol.* **2003**, *21*, 1166; b) A. Nel, T. Xia, L. Madler, N. Li, *Science* **2006**, *311*, 622.
[2] a) K. Haupt, *Analyst* **2001**, *126*, 747; b) P. R. Leroueil, S. Y. Hong, A. Mecke, J. R. Baker, B. G. Orr, M. M. B. Holl, *Acc. Chem. Res.* **2007**, *40*, 335.
[3] a) R. R. Henriquez, T. Ito, L. Sun, R. M. Crooks, *Analyst* **2004**, *129*, 478; b) X. Y. Xiao, A. J. Bard, *J. Am. Chem. Soc.* **2007**, *129*, 9610; c) Y. G. Zhou, N. V. Rees, R. G. Compton, *Angew. Chem.* **2011**, *123*, 4305; *Angew. Chem. Int. Ed.* **2011**, *50*, 4219.
[4] a) S. A. Bernhard, *J. Am. Chem. Soc.* **1952**, *74*, 4946; b) F. H. Dickey, *Proc. Natl. Acad. Sci. USA* **1949**, *35*, 3; c) S. A. Piletsky, A. P. F. Turner, *Electroanalysis* **2002**, *14*, 317.
[5] a) N. M. Bergmann, N. A. Peppas, *Prog. Polym. Sci.* **2008**, *33*, 271; b) A. Bossi, F. Bonini, A. P. F. Turner, S. A. Piletsky, *Biosens. Bioelectron.* **2007**, *22*, 1131.
[6] S. Koenig, V. Chechik, *Chem. Commun.* **2005**, 4110.
[7] S. C. Biradar, D. B. Shinde, V. K. Pillai, M. G. Kulkarni, *J. Mater. Chem.* **2012**, *22*, 10000.
[8] a) A. B. Moghaddam, T. Nazari, J. Badraghi, M. Kazemzad, *Int. J. Electrochem. Sci.* **2009**, *4*, 247; b) R. N. Singh, B. Lal, M. Malviya, *Electrochim. Acta* **2004**, *49*, 4605.
[9] a) A. Chevreau, B. Phillips, B. G. Higgins, S. H. Risbud, *J. Mater. Chem.* **1996**, *6*, 1643; b) J. Wouters, O. I. Lebedev, G. Van Tendeloo, H. Yamada, N. Sato, J. Vanacken, V. V. Moshchalkov, T. Verbiest, V. K. Valev, *J. Appl. Phys.* **2011**, *109*, 076105.
[10] F. Iskandar, M. Abdullah, H. Yoden, K. Okuyama, *J. Sol-Gel Sci. Technol.* **2004**, *29*, 41.
[11] a) H. Ai, S. A. Jones, Y. M. Lvov, *Cell Biochem. Biophys.* **2003**, *39*, 23; b) T. Cassagneau, T. E. Mallouk, J. H. Fendler, *J. Am. Chem. Soc.* **1998**, *120*, 7848.
[12] D. V. Novikov, *Russ. J. Appl. Chem.* **2008**, *81*, 153.
[13] a) L. H. Chen, A. Dudek, Y. L. Lee, C. H. Chang, *Langmuir* **2007**, *23*, 3123; b) Z. Matharu, A. J. Bandodkar, V. Gupta, B. D.

Malhotra, *Chem. Soc. Rev.* **2012**, *41*, 1363; c) H. J. Tsai, Y.-L. Lee, *Soft Matter* **2009**, *5*, 2962.
[14] a) H. M. Ding, P. Bertoncello, M. K. Ram, C. Nicolini, *Electrochem. Commun.* **2002**, *4*, 503; b) V. Vidya, N. P. Kumar, S. N. Narang, S. Major, S. Vitta, S. S. Talwar, P. Dubcek, H. Amenitsch, S. Bernstorff, *Colloids Surf. A* **2002**, *198*, 67.
[15] a) R. Capan, A. K. Hassan, A. V. Nabok, A. K. Ray, T. H. Richardson, M. C. Simmonds, C. Sammon, *IEE Proc-Circ. Dev. Syst.* **2003**, *150*, 367; b) L. Zhang, Y. Li, Y. Shen, A. Xie, *Mater. Chem. Phys.* **2011**, *125*, 522.
[16] a) D. K. Lee, Y. S. Kang, C. S. Lee, P. Stroeve, *J. Phys. Chem. B* **2002**, *106*, 7267; b) G. Tanami, V. Gutkin, D. Mandler, *Langmuir* **2010**, *26*, 4239.
[17] W. W. Focke, G. E. Wnek, Y. Wei, *J. Phys. Chem.* **1987**, *91*, 5813.
[18] N. Jaber, A. Lesniewski, H. Gabizon, S. Shenawi, D. Mandler, J. Almog, *Angew. Chem.* **2012**, *124*, 12390; *Angew. Chem. Int. Ed.* **2012**, *51*, 12224.

